Coherent control of photon-assisted tunneling between quantum dots: A theoretical approach using genetic algorithms

Ilia Grigorenko, Oliver Speer, and Martin E. Garcia*
Institut für Theoretische Physik der Freien Universität Berlin, Arnimallee 14, 14195 Berlin, Germany
(Received 14 January 2002; published 28 May 2002)

We analyze theoretically the electron tunneling induced by an ultrashort pulse of electric field between two metallic reservoirs coupled through a double quantum dot. We solve the equations of motion for the reduced density matrix to determine the transferred charge, which is a functional of the external field. Then, we use genetic algorithms to determine the optimal shape of the electric field that maximizes the transferred charge. Results show that, due to the presence of Rabi oscillations, a sequence of pulses of different shapes is needed. Such pulse sequence leads to a remarkable enhancement of the current with respect to a single (Gaussian or square) pulse. We analyze the cases of interdot Coulomb repulsion $U=0$ and $U\to\infty$.

DOI: 10.1103/PhysRevB.65.235309 PACS number(s): 73.40.Gk, 73.50.Pz

I. INTRODUCTION

Coherent control of carrier dynamics in mesoscopic systems using external ultrashort pulses of time-dependent fields has become a subject of active research in recent years.[1–4] In particular, the study of photon-induced and photon-suppressed quantum dynamical tunneling has attracted much attention due to the potential applications of these effects in quantum computing. Sequences of laser pulses of different durations affect the systems in different ways and permit one to perform some restricted manipulation of physical quantities, such as the photon-induced current.[2,3]

On the other hand, in atomic and molecular physics, the advent of pulse-shaping and feed-back techniques for the modulation of amplitude and phase of ultrashort laser pulses has opened the possibility of going a step further and teach the lasers to control occupations of electronic levels in atoms[5] or to drive molecular reactions in real time,[6–9] as proposed by Judson and Rabitz.[10] The idea consists in designing pulses or sequences of pulses having a given optimal shape (and phase) so that the desired nuclear wave-packet dynamics is induced. For instance, in experiments using self-learning algorithms on small clusters and molecules laser pulse profiles (and phases) were optimized in such a way that certain fragmentation or ionization channels could be favored and others were suppressed.[7–9] It is still an open question whether such nice examples of laser manipulation of wave-packet dynamics can be also performed in mesoscopic systems. For such systems, not the nuclear but the electronic degrees of freedom might offer the possibility of control by pulse shaping. An important requirement for the control of the wave-packet dynamics is the existence of phase coherence over a time range comparable to the duration of the pulse sequence. This condition is certainly fulfilled by mesoscopic systems such as quantum dots QD's, which are characterized by the spatial and temporal coherence of their electronic states.[11] For this reason quantum dots are often referred as ''artificial atoms,''[12] and double quantum dots as ''artificial molecules.''[13]

In this paper we provide a theoretical description of a coherent manipulation of photon-assisted tunneling in quantum dots via optimization of external control fields. We show for a model system that measurable quantities, such as the photon-induced current, can be considerably enhanced if optimized time-dependent electric fields are used.

As model device we consider an electron pump based on resonant photon-assisted tunneling through a double quantum dot.[14] A periodic external field applied on this pump induces spatial Rabi oscillations that make possible electron delocalization and transport, otherwise inhibited.[14] This system shows interesting time-dependent tunneling dynamics.[15]

To achieve the pulse shaping or optimization of the external fields we use genetic algorithms, as proposed in Ref. 10. The genetic algorithm (GA) belongs to a new generation of the so-called intelligent global optimization techniques. First proposed by Holland[16] in connection with his theory of adaptive systems, it has been applied to numerous difficult optimization problems, particularly in engineering and applied sciences.[17,18] This search method has been recently applied to optimize the atomic structures of small clusters[19–21] and also to obtain ground-state functions of quantum systems.[22,23]

We show in this paper how the GA allows a fast and efficient search of the optimal time-dependent field. Our results indicate that, due to the complex photon-assisted electron dynamics in the electron pump, involving Rabi oscillations with frequencies changing in time, pulse sequences of complicated shape are needed to induce a maximal current.

The paper is organized as follows. In Sec. II we present the theoretical model for both the description of the electron pump and the pulse shaping. In Sec. III we show and discuss the results. Finally, in Sec. IV we present a summary and outlook of further possible applications.

II. THEORY

A. Model Hamiltonian and equations of motion

We consider a device consisting in a double quantum dot coupled to two metallic leads (reservoirs) and configured as an electron pump as described in Ref. 14. This device is illustrated in Fig. 1. The double quantum dot can be modeled by only two nondegenerated and weakly coupled electron

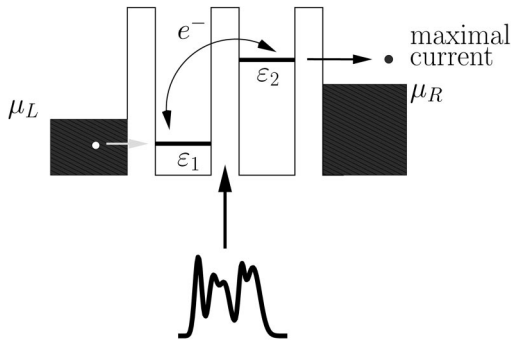

FIG. 1. Illustration of the photon-assisted tunneling via optimization of the shape of the external electric pulse on an electron pump. An external field of optimized shape excites a double QD between two metallic contacts. The resulting charge-exchange process leads to a maximal current.

levels with energies ε_1 and ε_2. This simplification is allowed in the resonant approximation. The quantum dot 1 is connected to the reservoir on the left, and the second quantum dot is coupled to the right reservoir. The applied voltage is biased in such a way that the chemical potential of the left reservoir μ_L is lower than that on the right reservoir (μ_R). Therefore, in absence of external perturbation the level 1 is occupied whereas level 2 is empty. Since we also assume that the coupling between the quantum dots is very weak, no current flows in the absence of external fields.

If the external resonant electric field is applied to the system, it works as a pump: Rabi oscillations of the electron occupations occur between the levels 1 and 2, and electrons can tunnel from the left to the right reservoir.[14,15]

The Hamiltonian of the double QD coupled to the external field can be expressed as

$$H_{DQD}=\sum_{i=1}^{2}\varepsilon_i(t)c_i^\dagger c_i+d(c_1^\dagger c_2+c_2^\dagger c_1), \tag{1}$$

where $c_i^\dagger$ (c_i) is the creation (annihilation) operator for an electron on dot i. $\varepsilon_i(t)=(-1)^i/2\ [\Delta\varepsilon+A(t)\cos\omega t]$. $\Delta\varepsilon=\varepsilon_2-\varepsilon_1$ is the energy difference between the on-site energies of the quantum dots. The intradot interactions are absorbed in the on-site energies. $A(t)\cos\omega t$ is the time-varying external field, which causes the on-site energies to oscillate against each other. The amplitude $A(t)$ is also time dependent and describes the pulse shape. The external field is applied only to the dots.[14] d is the coupling between the QD's.

The Hamiltonian for the metallic reservoirs and the tunnel barriers is given by[14]

$$H_{RT}=\sum_{\mathbf{k}\in l/l=L,R}\varepsilon_{\mathbf{k}l}c_{\mathbf{k}l}^\dagger c_{\mathbf{k}l}+\sum_{\mathbf{k}\in L}V_{\mathbf{k}L}(c_{\mathbf{k}L}^\dagger c_1+c_1^\dagger c_{\mathbf{k}L})$$
$$+\sum_{\mathbf{k}\in R}V_{\mathbf{k}R}(c_{\mathbf{k}R}^\dagger c_2+c_2^\dagger c_{\mathbf{k}R})+Un_1n_2. \tag{2}$$

Here, $c_{\mathbf{k}l}^\dagger$, with $l=L,R$ creates an electron of momentum $\mathbf{k}$ in reservoir l. The quantities $V_{\mathbf{k}li}$, with $l=L,R$, and $i=1,2$ represent the tunnel matrix elements between the reservoirs and the QD's. U is the magnitude of the interdot electron-electron repulsion, and the occupation operators n_1 and n_2 are given by $n_1=c_1^\dagger c_1$ and $n_2=c_2^\dagger c_2$. For simplicity, spin is neglected.

In the derivation of Eqs. (3) we have performed the following approximation. We assume that the reservoir on the right has a broadband of unoccupied states, so that once an electron has jumped from the second quantum dot to the reservoir it cannot jump back any more. Thus, the time scale for the tunneling process between the second dot and the reservoir on the right is determined by a transfer rate $\Gamma_2=2\pi\rho_R(\varepsilon)|V_{\mathbf{k}R}|^2$, where ρ_R is the density of states in the right reservoir. Similarly, the transfer rate Γ_1 is given by $\Gamma_1=2\pi\rho_L(\varepsilon)|V_{\mathbf{k}L}|^2$.

In order to describe the electron dynamics we use a density-matrix approach similar to that derived in Ref. 24. Given the above Hamiltonians, the master equation for density matrix ρ, which describes the evolution of the system, reads

$$i\hbar\frac{\partial}{\partial t}\rho_{11}=i\Gamma_1\rho_0+d(\rho_{12}-\rho_{21}),$$
$$i\hbar\frac{\partial}{\partial t}\rho_{22}=-i\Gamma_2\rho_{22}+d(\rho_{21}-\rho_{12}), \tag{3}$$
$$i\hbar\frac{\partial}{\partial t}\rho_{12}=-i\frac{\Gamma_2}{2}\rho_{12}+2\varepsilon_1(t)\rho_{12}+d(\rho_{22}-\rho_{11}),$$
$$i\hbar\frac{\partial}{\partial t}\rho_{21}=-i\frac{\Gamma_2}{2}\rho_{21}+2\varepsilon_2(t)\rho_{21}+d(\rho_{22}-\rho_{11}).$$

Equations (3) allow one to investigate the case of zero and infinite interdot Coulomb repulsion U by choosing the proper expression for the quantity ρ_0. For $U=0$ we write $\rho_0=1-\rho_{11}$, whereas the case $U\to\infty$ requires $\rho_0=1-\rho_{11}-\rho_{22}$, which projects out double occupancies.[24] The initial situation is $\rho_{11}=1$, $\rho_{22}=0$, as can be inferred from Fig. 1. We consider photon assisted tunneling when the resonance condition $\hbar\omega=\sqrt{(\Delta\varepsilon)^2+4d^2}$ is satisfied.

From the integration of Eqs. (3) one can obtain the charge transferred from the left into the right reservoir due to the action of the external field over the time interval $[0,T]$. For that purpose we write the current operator $\hat{J}=id/\hbar(c_1^\dagger c_2-c_2^\dagger c_1)$, which leads, in combination with Eqs. (3), to the time-dependent average current

$$\langle I(t)\rangle=e\,\mathrm{Tr}\{\hat{\rho}\hat{J}\}=e\frac{\partial\rho_{22}(t)}{\partial t}+\frac{e\,\Gamma_2}{\hbar}\rho_{22}(t), \tag{4}$$

where e is the electron charge. The net transferred charged Q_T is obtained as

$$Q_T=\int_o^T dt\langle I(t)\rangle=\frac{e\,\Gamma_2}{\hbar}\int_0^T dt\,\rho_{22}(t)+e\,\rho_{22}(T). \tag{5}$$

Obviously, Q_T only represents the transferred charge to the right reservoir when $\Gamma_2\neq 0$. In Eq. (5), the second term indicates that, after the field is switched off ($t>T$), the charge remaining in the second quantum dot $e\,\rho_{22}(T)$ is completely transferred to the right reservoir.

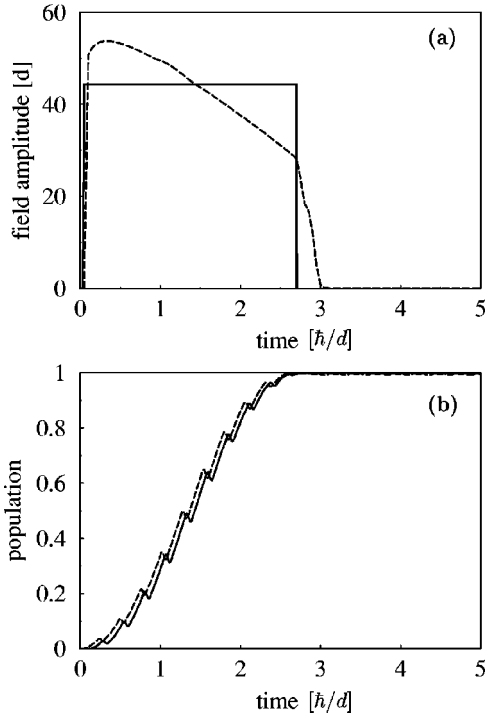

FIG. 2. Optimization of the external field for the isolated double quantum dot ($\Gamma=0$). (a) Solid line: reference pulse of duration $\tau=\pi\Omega_{max}^{-1}$, intensity A_0 yielding the first maximum of $J_1(A_0/\hbar\omega)$ (see text), and energy E_0. Dashed line: optimal pulse shape for the maximization of the charge transferred from the left to the right quantum dot. The pulse energy is E_0. (b) Corresponding time dependence of the occupation $\rho_{22}(t)$ on the second dot for the pulses shown in (a).

It is important to point out that $Q_T=Q_T[A(t)]$ is a functional of the field amplitude $A(t)$, and can exhibit different types of behavior depending on the form of $A(t)$. For instance, if the external field has a Gaussian shape $A(t)=A_0\exp(-t^2/2\tau^2)$ of duration τ, then Q_T shows Stückelberg-like oscillations as a function of τ.[15] However, the Gaussian shape of $A(t)$ does not necessarily maximize the transferred charge. Our goal is to find the optimal pulse shape $A_{opt}(t)$, which maximizes Q_T, i.e., which satisfies $Q_T^{max}=Q_T[A_{opt}(t)]$.

B. Determination of the optimal field

The problem of finding $A_{opt}(t)$ is very complicated because of its high nonlinearity and the large number of degrees of freedom. Therefore, we use a global search method: GA. The GA was developed to optimize (maximize or minimize) a given property, depending on many variables of the system. In GA language the quantity to optimize is referred as the fitness function. The GA basically maps the degrees of freedom or variables of the system to be optimized onto a genetic code (represented by a vector). Thus, a random population of individuals is created as a first generation. This population ''evolves'' and subsequent generations are reproduced from previous generations through application of different operators on the genetic codes, like, for instance, mutations, crossovers, and reproductions or copies. The mutation operator changes randomly the genetic information of an individual, i.e., one or many components of the vector representing its genetic code. The crossover or recombination operator interchanges the components of the genetic codes of two individuals.[18] In a simple recombination, a random position is chosen at which each partner in a particular pair is divided into two pieces. Each vector then exchanges a section of itself with its partner. The copy or reproduction operator merely transfers the information of the parent to an individual of the next generation without any changes.

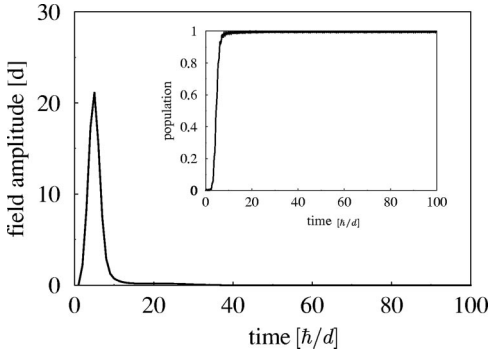

FIG. 3. Optimization of the external field for the isolated double quantum dot using constraints for the minimum pulse width. Optimal pulse shape for the maximization of the charge transferred from the left to the right quantum dot. Pulse energy $E=0.57E_0$ $\Gamma=0$. Inset: corresponding time dependence of the occupation $\rho_{22}(t)$ on the second dot.

In our present approach the vector representing the genetic code is just the pulse shape $A(t)$. The fitness function, i.e., the functional to be maximized by the successive generations is the transferred charge $Q_T[A(t)]$ [see Eq. (5)]. The genetic algorithm applied to pulse shaping consists in the following steps.

(i) We create a random initial population $\{A_j^{(0)}(t)\}$, $j=1,\ldots,N$, consisting of N different pulse amplitudes $A_j^{(0)}(t)$.

(ii) The fitness $Q_T[A_j^{(0)}(t)]$ of all individuals is determined.

(iii) A new population $\{A_j^{(1)}(t)\}$ is created through application of the genetic operators.

(iv) The fitness of the new generation is evaluated.

(v) Steps (iii) and (iv) are repeated for the successive generations $\{A_j^{(n)}(t)\}$ until convergence is achieved and the optimal pulse shape that maximizes Q_T is found.

It is important to indicate that the crossover and mutation operations usually used would produce discontinuous pulses, which are, of course, not realistic. In order to avoid this problem we use the so-called smooth or uncertain crossover and mutation operations.[22,23] An example of a smooth crossover operation is performed in the following:

$$A_1^{(n+1)}(t)=A_1^{(n)}(t)St(t)+A_2^{(n)}(t)[1-St(t)],$$

$$A_2^{(n+1)}(t)=A_2^{(n)}(t)St(t)+A_1^{(n)}(t)[1-St(t)], \qquad (6)$$

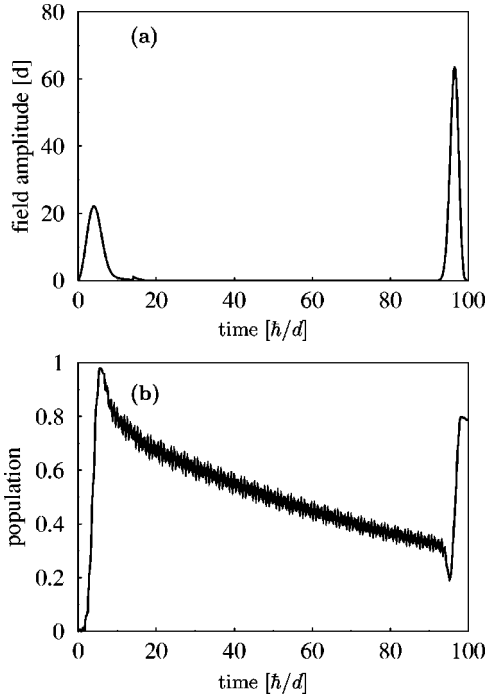

FIG. 4. Optimization for the electron pump ($\Gamma \neq 0$). (a) Optimal pulse shape that induces maximal current for $\Gamma = 0.01d$. Pulse energy $E = 4.26E_0$ (b) Corresponding behavior of $\rho_{22}(t)$.

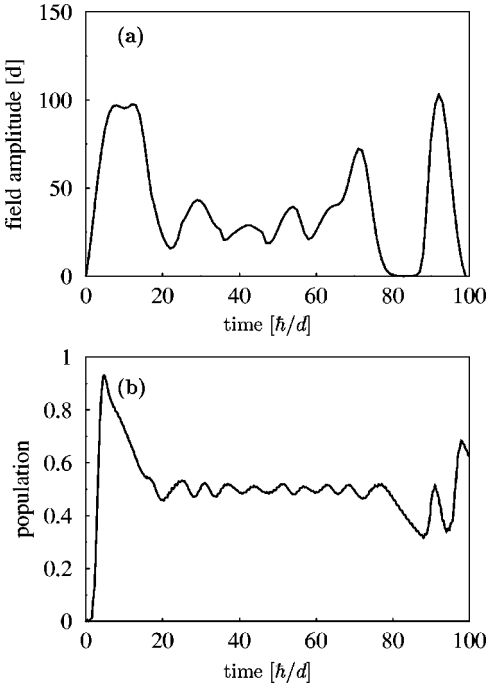

FIG. 5. Optimization for the electron pump ($\Gamma \neq 0$). (a) Optimal pulse shape for $\Gamma = 0.05d$. Pulse energy $E = 121E_0$ (b) Corresponding behavior of $\rho_{22}(t)$.

where $St(x)$ is a smooth step function of the form $St(t) = [1 + \tanh(t - t_0)/k_c^2]/2$. t_0 is chosen randomly [$t_0 \in (0,T)$] and k_c is a parameter that controls the sharpness of the crossover operation.

We assume that the control field is active within time interval $t \in [0,T]$, with boundary conditions $A(0) = A(T) = 0$. As initial population of field amplitudes satisfying the boundary conditions we choose Gaussian-like functions of the form

$$A_j^{(0)}(t) = I_j^0 \exp[-(t - t_j)^2/\tau_j^2] t(t - T) \tag{7}$$

with random values for $t_j \in [0,T]$ and the duration $\tau_j \in [0,T]$. The peak intensity I_j^0 for each pulse is calculated from the condition that all pulses must carry the same energy

$$E_0 = \int_0^T A^2(t) \cos^2 \omega t \, dt. \tag{8}$$

Equation (8) represents a constraint for our calculations.

III. RESULTS

In this section we present results of the optimization of the transferred charge in the system. The parameters used in our calculations are given in terms of the tunneling matrix element d. The energy difference $\Delta\varepsilon = \varepsilon_2 - \varepsilon_1$ must be much larger than d to ensure that the ground state of the double quantum dot is localized on the left side and the excited state is localized on the right side. This also leads to a sharper resonance behavior. Therefore we set $\Delta\varepsilon = 24d$. In our calculations we use symmetric coupling of the QD to the reservoirs $\Gamma_1 = \Gamma_2 \equiv \Gamma$ and compute optimal field shape for different values of the coupling constants $\Gamma = 0, 0.01d, 0.05d$. It is important to point out that Γ must be smaller than d so that the Rabi oscillations do not become overdamped. If Γ is large the system saturates very rapidly to $\rho_{11} = \rho_{22} = 1/2$ and no interesting transient dynamics can be observed. Finally, we choose the control interval $T = 100\hbar/d$, which is large enough to allow back and forth motion of the electrons between the quantum dots and is of the order of $\hbar/\Gamma$.

We discuss first results for $U = 0$, i.e., neglecting the interdot Coulomb repulsion.

The search for the optimal pulse in the system described

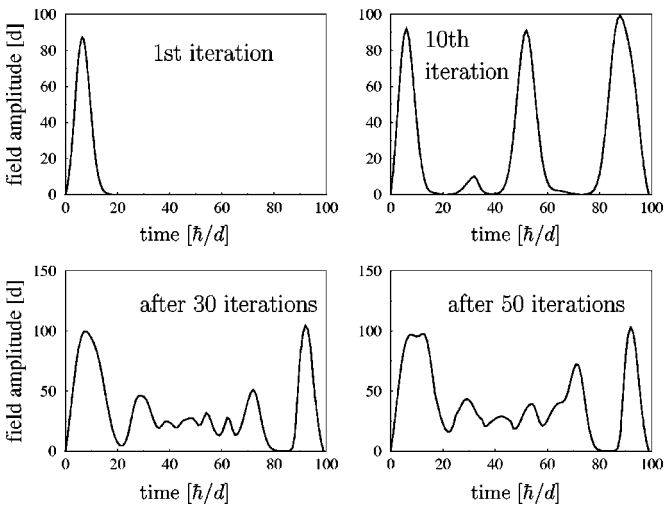

FIG. 6. Illustration of the optimization process using genetic algorithms. Evolution of the ''fittest'' pulse shape for maximization of the current for $\Gamma = 0.05d$.

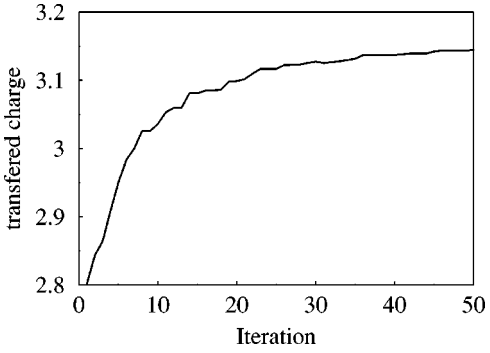

FIG. 7. Evolution of the transfered charge for increasing number of iteration of the GA for $\Gamma = 0.05d$.

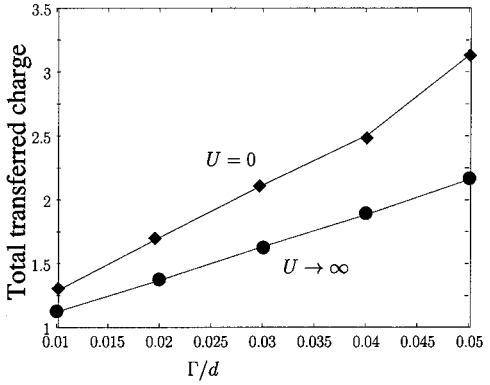

FIG. 8. Dependence of the total transferred charge Q_T (diamonds) induced by the optimal pulse as a function of the coupling Γ to the leads for $U=0$. The circles represent the values of Q for $U \to \infty$.

in Sec. II constitutes a difficult task. From the elementary analysis of Eqs. (3) it is clear that the optimal pulse should first be able to transfer an electron from left to the right QD (inversion of the occupation) and then to keep this situation as long as possible. However, there are many different pulse shapes able to achieve this situation, and it is *a priori* not clear which one maximizes Q_T.

For $\Gamma = 0$, for example, Eqs. (3) can be solved analytically for some cases. If, for example, the external field is periodic in time $A(t) = A_0 \cos \omega t$, with a constant amplitude A_0, an electron placed on one of the dots will oscillate back and forth between the dots with the Rabi frequency $\Omega = 2d/\hbar\, J_1(A_0/\hbar\omega)$,[25,26] J_1 being the Bessel function of order 1, if the system absorbs one photon. In order for this to happen, ω must fulfill the resonance condition $\hbar\omega = \sqrt{\Delta\varepsilon^2 + 4d^2}$. The description of the tunneling dynamics for pulses of varying intensity is much more complicated, because the Rabi frequency changes in time.

Thus, for pulses of constant amplitude there is an upper limit Ω_{max} for the Rabi frequency, which is obtained when the ratio $x = A_0/\hbar\omega$ is such that the function $J_1(x)$ has its first maximum. Using this property we construct a reference pulse of square shape [$A(t) = A_0$ for $0 \leqslant t \leqslant \tau$ and $A(t) = 0$ otherwise] with intensity A_0 as defined above and duration $\tau = \pi\Omega_{max}^{-1}$. In the following, we will use the energy E_0 of such reference pulse as a unit of pulse energies. In principle, one would expect that the reference pulse defined above exactly achieves an inversion of the occupation in the double quantum dot within the shortest time (assuming only one-photon absorption). However, as we show below, such a pulse shape is not the optimal one.

In Fig. 2 we compare the effect induced on the isolated double quantum dot ($\Gamma = 0$) by the reference square pulse with that induced by the optimal one calculated using GA and having the same energy E_0. As one can see in Fig. 2(b), GA finds a pulse shape that induces a slightly faster transfer of the charge.

Note that, if no constraints are imposed on the width of the pulses, a pulse of infinitely small width (δ pulse) should yield to the maximal Q_T. Such pulse would produce $\rho_{22}(t) = 1$ over the whole time control interval, leading to the maximum possible value $Q_T^{max} = eT\Gamma/\hbar + e$. However, the energy of such pulse would diverge. Pulses with zero width and infinite energy cannot describe a realistic situation. Moreover, for such pulses the whole model would break down, since very energetic pulses would excite many levels on each quantum dot.

In the following calculations we set the time interval for charge transfer $T = 100\hbar/d$. We also put a constraint on the minimal width of the pulse in order to describe pulses that can be achieved experimentally. In our calculations this minimal width is naturally determined by the discretization of the time interval and by the smoothness parameters k_c and k_m of the crossover and mutation operations [see Eq. (6)].

In Fig. 3 we show the optimized pulse shape for the maximization of the charge transfer in the isolated double quantum dot ($\Gamma = 0$) under the constraint discussed above. The optimal pulse excites the system at the beginning of the control time interval, inducing an inversion of the occupation. $\rho_{22}(t)$ reaches the value 1 when the pulse goes to zero. Since $\Gamma = 0$ this occupation remains constant in time. As a consequence Q_T is maximized. From the comparison between Fig. 2(a) and Fig. 3 we see that a limitation of the minimal pulse width leads to more symmetric pulses. The corresponding evolution of the occupation of the second quantum dot is shown in the inset of Fig. 3.

In Fig. 4 we show the optimal field envelope and the induced occupation $\rho_{22}(t)$ in the case of the weak coupling to reservoirs with coupling constant $\Gamma = 0.01d$. Note that the optimal field is structured as a sequence of two pulses. The first one acts at the beginning and has the proper shape to bring the occupation of the second QD to a value close to 1. However, since $\Gamma \neq 0$ and according to Eqs. (3), $\rho_{22}(t)$ starts to decrease as soon as the first pulse goes to zero [see Figs. 4(a) and 4(b)]. Shortly before the end of the control time interval the second pulse brings the occupation $\rho_{22}(t)$ again to a high value [Fig. 4(b)]. The structure of the optimal pulse can be easily interpreted with the help of the expression of Q_T as a functional of $\rho_{22}(t)$ [Eq. (5)]. The first pulse tends to keep the term $e\Gamma_2/\hbar \int_0^T dt\, \rho_{22}(t)$ as large as possible, whereas the second pulse acts to increase $e\rho_{22}(T)$. As a consequence, Q_T is maximized.

Figure 5 shows results for the same system, but with

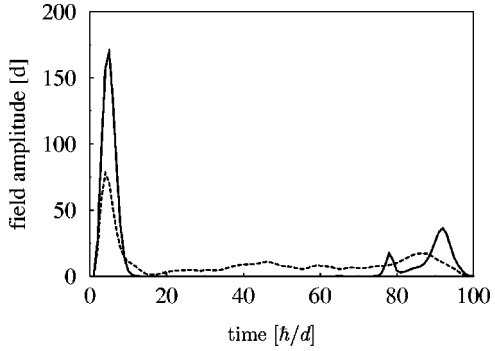

FIG. 9. Optimized pulse form for $\Gamma = 0.01d$ (solid line, pulse energy $E = 48.4E_0$) and $\Gamma = 0.05d$ (dashed line, pulse energy $E = 13E_0$) for the maximization of the average occupation P_{22} of the second quantum dot (see text).

larger coupling constant, namely, $\Gamma = 0.05d$. As can be seen in Fig. 5(a), in this case the optimal solution exhibits not only pulses at the beginning and at the end of the control interval, but also a complicated sequence of pulses between them, which prevent $\rho_{22}(t)$ to go to zero and stabilize it around the value 1/2, i.e., at the state where both dots are equally occupied [Fig. 5(b)].

If Γ is increased further, the structure in the middle of the time interval becomes more important. In the limit of large Γ we expect a square pulse to maximize Q_T, since in this case the pulse only needs to transfer charge at some constant rate with a value of the order of Γ.

In order to illustrate the progress achieved by the genetic algorithm during the optimization process we show in Fig. 6 the shapes (envelopes) of the fittest pulses at different stages of the genetic evolution, for the case of $\Gamma = 0.05d$. In Fig. 6(a) one of the pulses of the initial population (parents) is plotted. As all other parents, this pulse is Gaussian-like and induces a net charge transfer of less than 1 electron. The successive application of the genetic operations improves the pulse shape and transforms the initial Gaussians in different pulse sequences. As a result, the envelope of the fittest pulse of the tenth generation [Fig. 6(b)], for instance, exhibits several peaks. After 30 iterations [Fig. 6(c)] the pulse form already exhibits most of the features of the optimal pulse, and after 50 iteration it converges to the optimal one [Fig. 6(d)]. To illustrate this convergence, we show in Fig. 7 the evolution of the transfered charge $Q_T[A(t)]$ as a function of the number of iterations of the GA. It is clear that after about 50 iterations the pulse induces a transferred charge very close to the optimal one.

In order to investigate the influence of the interdot Coulomb repulsion U we perform calculations similar to those described above, but for the case $U \to \infty$ using the same set of coupling parameters Γ. We found that the repulsion between QD's leads to a relatively smaller net transfered charge [see (Fig. 8)]. This is due to the fact that $U \to \infty$ prevents double occupancies in the system. Therefore, an electron from the left reservoir can jump into the double quantum dot only when the previous electron has already left the system and was transferred to the right reservoir.

TABLE I. Total transferred charge $Q_T[A(t)]$ for different pulses having different shapes but the same energy $E = 4.26E_0$ (see text). The coupling to the leads is assumed to be $\Gamma = 0.01d$ and the interdot repulsion $U = 0$.

Pulse shape	Q_T
Optimal pulse [see Fig. 4(a)]	1.29
Rectangular pulse	0.85
Gaussian pulse	0.74
Constant pulse	0.77

For the sake of comparison we have also calculated the optimal pulse shape, which maximizes the mean occupation of the second QD, using as fitness function the time integral of the occupation on the second quantum dot, $P_{22} = \int_0^T dt\, \rho_{22}(t)$ (for $\Gamma = 0.01d, 0.05d$). Interestingly, the optimal pulse also has two peak structures (Fig. 9). Indeed, the first pulse pumps one electron from the left to the right QD. The reason for the position of the second pulse is that its efficiency in increasing $\rho_{22}(t)$ is maximal when $\rho_{22}(t)$ reaches its minimum, i.e., at the end of the control interval.

Finally, and in order to show that pulse shaping can indeed lead to a remarkable enhancement of the photon-assisted current through double quantum dots, we indicate in Table I the values of the transferred charge Q_T for $\Gamma = 0.01d$ and pulses having different shapes $A(t)$ but carrying the same energy E. As expected, the optimal pulse found by the GA [already shown in Fig. 4(a)] induces clearly more transferred charge than pulses having other shapes. It is important to point out that the rectangular and Gaussian pulses mentioned in Table I are the fittest ones among rectangular and Gaussian pulses, respectively. Thus, the optimal pulse induces 1.74 times more charge than the best Gaussian pulse, and 1.5 times more charge than the best rectangular pulse. This shows that GA is a powerful method for solving the optimal control problem for the quantum systems on a finite interval of time.

IV. SUMMARY

We have presented a theoretical study of the optimal control of photon-assisted tunneling. We have shown that, as is the case for real molecules, pulse-shaping techniques could lead to an efficient control of wave-packet dynamics also in artificial molecules, such as double quantum dots. Of course, in the latter case ultrashort pulses of external fields must be created to manipulate the electron dynamics, unlike the case of real molecules, for which femtosecond laser pulses are used to control the nuclear wave-packet dynamics.

ACKNOWLEDGMENTS

This work has been supported by the Deutsche Forschungsgemeinschaft through Grant No. SFB 450.

*Corresponding author. Email address: garcia@physik.fu-berlin.de

[1] N.H. Bonadeo, J. Erland, D. Gammon, D. Park, D.S. Katzer, and D.G. Steel, Science **282**, 1473 (1998); G. Chen, N.H. Bonadeo, D.G. Steel, D. Gammon, D.S. Katzer, D. Park, and L.J. Sham, *ibid.* **289**, 1906 (2000); D. Gammon, N.H. Bonadeo, G. Chen, J. Erland, and D.G. Steel, Physica E (Amsterdam) **9**, 99 (2001).

[2] A.P. Heberle, J.J. Baumberg, and K. Köhler, Phys. Rev. Lett. **75**, 2598 (1995); A.P. Heberle, J.J. Baumberg, T. Kuhn, and K. Köhler, Physica B **272**, 360 (1999).

[3] B.E. Cole, J.B. Williams, B.T. King, M.S. Sherwin, and C.R. Stanley, Nature (London) **410**, 60 (2001).

[4] E. Dupont, P.B. Corkum, H.C. Liu, M. Buchanan, and Z.R. Wasilewski, Phys. Rev. Lett. **74**, 3596 (1995).

[5] V. Blanchet, M.A. Bouchene, and B. Girard, J. Chem. Phys. **108**, 4862 (1998).

[6] C.J. Bardeen, V.V. Yakovlev, K.R. Wilson, S.D. Carpenter, P.M. Weber, and W.S. Warren, Chem. Phys. Lett. **280**, 151 (1997).

[7] A. Assion, T. Baumert, M. Bergt, T. Brixner, B. Kiefer, V. Seyfried, M. Strehle, and G. Gerber, Science **282**, 919 (1998).

[8] S. Vajda, A. Bartelt, E.V. Kaposta, T. Leisner, C. Lupulescu, S. Minemoto, P. Rosendo-Francisco, and L. Woste, Chem. Phys. **267**, 231 (2001).

[9] T. Hornung, R. Meier, D. Zeidler, K.L. Kompa, D. Proch, and M. Motzkus, Appl. Phys. B: Lasers Opt. **B71**, 277 (2000); T. Hornung, R. Meier, R. de Vivie-Riedle, and M. Motzkus, Chem. Phys. **267**, 261 (2001).

[10] R.S. Judson and H. Rabitz, Phys. Rev. Lett. **68**, 1500 (1992).

[11] See, for example, *Mesoscopic Phenomena in Solids*, edited by B. L. Altshuler, P. A. Lee, and R. Webb (Elsevier, Amsterdam, 1991).

[12] R. Ashoori, Nature (London) **379**, 413 (1996).

[13] R.H. Blick, R.J. Haug, J. Weis, D. Pfannkuche, K.v. Klitzing, and K. Eberl, Phys. Rev. B **53**, 7899 (1996).

[14] C.A. Stafford and N.S. Wingreen, Phys. Rev. Lett. **76**, 1916 (1996).

[15] O. Speer, M.E. Garcia, and K.H. Bennemann, Phys. Rev. B **62**, 2630 (2000).

[16] J.H. Holland, *Adaptation in Natural and Artificial Systems* (University of Michigan, Ann Arbor, MI, 1975).

[17] R. Matthews, New Sci. **148**, 41 (1995).

[18] P. Sutton and S. Boyden, Am. J. Phys. **62**, 549 (1994).

[19] R.S. Judson, M.E. Colvin, J.C. Meza, A. Huffer, and D. Gutierrez, Int. J. Quantum Chem. **44**, 277 (1992).

[20] D.M. Deaven and K.M. Ho, Phys. Rev. Lett. **75**, 288 (1995).

[21] I.L. Garzon, K. Michaelian, M.R. Beltran, A. Posada-Amarillas, P. Ordejon, E. Artacho, D. Sanchez-Portal, and J.M. Soler, Phys. Rev. Lett. **81**, 1600 (1998).

[22] I. Grigorenko and M.E. Garcia, Physica A **284**, 131 (2000).

[23] I. Grigorenko and M.E. Garcia, Physica A **291**, 439 (2001).

[24] T.H. Stoof and Y.V. Nazarov, Phys. Rev. B **53**, 1050 (1996).

[25] Y.B. Zeldovich, Sov. Phys. JETP **24**, 1006 (1967).

[26] P.K. Tien and J.P. Gordon, Phys. Rev. **129**, 647 (1963).